

Noise-Induced Thermalization in Quantum Systems

Sameer Dambal,^{1, 2, *} Yu Zhang,¹ Eric R. Bittner,² and Pavan Hosur^{2, 3, †}

¹*Theoretical Division, Los Alamos National Laboratory, Los Alamos, NM, 87544, USA*

²*Department of Physics, University of Houston, Houston, TX 77204, USA*

³*Texas Center for Superconductivity, University of Houston, Houston, Texas 77204, United States*

In the current Noisy Intermediate-Scale Quantum era, noise is widely regarded as the primary obstacle to achieving fault-tolerant quantum computation. However, certain stages of the quantum computing pipeline can, in fact, benefit from this noise. In this work, we exploit the Eigenstate Thermalization Hypothesis to show that noise generically accelerates a fundamental task in quantum computing – the preparation of Gibbs states. We demonstrate this behavior using classical and quantum simulations with Haar-random and phase-flip noise, respectively, on a spin-1/2 chain with a local Hamiltonian. Our non-integrable model sees $\sim 3.5x$ faster thermalization in the presence of noise, while our integrable model, which would not otherwise thermalize, reaches a thermal state due to noise. Since certifying a local Gibbs state is relatively easy on a quantum computer, our approach provides a new practical solution to a key problem in quantum computing. More broadly, these results establish a new paradigm in which noise can be harnessed on quantum computers, enabling practical advantages before the years of fault-tolerance.

I. INTRODUCTION

Quantum simulation [1] is heralded as one of the early applications of fault-tolerant quantum computers, dating back to Richard Feynman’s proposal in 1982 [2]. As we stand today, the predicted applications of such a technology has vastly expanded to enhancing secure communications [3] (quantum communications), improving sensitivity to measurements [4] (quantum sensing), tightening cryptographic protocols [5] (quantum cryptography), learning problems in quantum machine learning (QML) [6–8], and speeding up optimization problems [9, 10], among others. Across these disparate avenues, the first step common to all them is the accurate preparation of initial states. Depending on the problem at hand, these could be ground states as required in quantum annealing [10] or, more commonly, thermal/Gibbs states as required in quantum machine learning, quantum Mpemba effect [11], adiabatic quantum computing [12–14], quantum thermodynamics [15, 16], and many systems that simulate equilibrium physics. In fact, in QML, Boltzmann machines are defined by thermal states and training them requires repeatedly preparing Gibbs states of parametrized Hamiltonians. Efficient Gibbs state preparation, therefore, directly determines the feasibility and scalability of quantum Boltzmann machines.

Several techniques have been developed for sampling these states on quantum circuits. A non-exhaustive list includes quantum rejection sampling from an infinite temperature state [17], mixing using quantum walks [18], dynamical simulation of system-bath interactions [19, 20], imaginary time evolution [21], etc. In addition,

numerous variational quantum algorithms have also been proposed [22–24] and demonstrated experimentally [25, 26]. However, since these states are mixed and reflect classical probability distributions, preparing them becomes a non-trivial task. In low temperatures, this process is as hard as preparing ground states, and may require exponentially long times for its generation. The latter is known to be a QMA-hard problem [27] and therefore motivates experimental efforts to accelerate thermalization [28]. To further circumvent challenges arising from preparing mixed states on quantum circuits, researchers have explored two complementary directions: generating thermalization dynamics in closed quantum systems [29, 30], and developing quantum algorithms that estimate thermal expectation values using pure states [31]. These ideas have also been demonstrated experimentally in Ref. [32].

Despite these advances in both theory and experiments, noise continues to stand as one of the main impediments to derive quantum advantage in the current Noisy Intermediate-Scale Quantum (NISQ) era. This adversity impacts various stages of the quantum computing pipeline, ranging from state preparation, evolution, and measurement. It corrupts quantum computations, drives decoherence, and sets a limited timescale to run useful and advantageous computations. Researchers have developed several strategies to fight these adversities, including quantum error correction [33], error mitigation [34, 35], dynamical decoupling [36, 37], etc. These approaches aim to correct, suppress, or cancel noise so that circuits can run reliably.

While these efforts continue to show promising results to realize fault-tolerance, noise still persists as a major bottleneck, demanding a lot of time and resources across all sectors of the quantum computing (QC) community. In this work, we flip this perspective and ask the question, *”Can this noise be used constructively in the QC*

* sadambal@central.uh.edu

† phosur@central.uh.edu

pipeline?”. To answer this in the affirmative, we present a protocol that uses noise to accelerate the preparation of localized Gibbs states within a many-body pure state of a NISQ device. In particular, strongly correlated quantum systems display chaotic dynamics owing to the non-integrability of the Hamiltonian. When such a Hamiltonian is implemented on a NISQ device, the long-time expectation of certain local observables begin to resemble those derived from equilibrium statistical ensembles in the thermodynamic limit [38]. Specifically,

$$\langle \psi(t) | O | \psi(t) \rangle = \frac{\text{Tr}[O e^{-\beta H}]}{Z} \quad (1)$$

where $Z = \text{Tr}[e^{-\beta H}]$ is the partition function and O is a real space local observable. Garrison and Grover [39] argue that for Eq. (1) to hold, the reduced density matrix over partitioned subspaces A, B of a quantum system must satisfy,

$$\rho_A = \frac{\text{Tr}_{\bar{A}}[e^{-\beta H}]}{\text{Tr}[e^{-\beta H}]} \quad (2)$$

$$\approx \frac{e^{-\beta H_A}}{\text{Tr}_A[e^{-\beta H_A}]} \quad (3)$$

with vanishing contributions in the thermodynamic limit. Deutsch [40] argued that the entanglement entropy of the smaller system equals its thermodynamic entropy, indicating the formation of localized Gibbs states in strongly correlated Hamiltonians. More intuitively, one can think of the subsystem treating its complement as the bath with which it exchanges information and relaxes to a Gibbs state. These ideas are collectively called the Eigenstate Thermalization Hypothesis (ETH) and they explore thermalization dynamics in closed quantum systems. For more intuition, we invite the readers to peruse the pioneering works by Deutsch [41] and Srednicki [42, 43] for an operator version of ETH, and Refs. [40, 44–47] for a more state-based narrative rooting from the Ergodic Bipartition.

Taking inspiration from these ideas, we propose that when noise is interleaved between Hamiltonian dynamics, it induces a degree of non-integrability and chaos, and enhances the rate of Gibbs state preparation. More specifically, we propose the following noise protocol,

$$\mathcal{E}(\rho) = \mathcal{N} \cdot \rho_0 \cdot \mathcal{N}^\dagger \quad (4)$$

where $\mathcal{N} = U(t_{max} - t_{max-1})M \cdots U(t_2 - t_1)MU(t_1)$, $U(t_n - t_{n-1}) = e^{-iH(t_n - t_{n-1})}$ and M is an operator that introduces noise as “shocks” interleaved between unitary dynamics. Here, H is any non-integrable Hamiltonian and $\rho_0 = |\psi_0\rangle\langle\psi_0|$ is the initial density matrix.

Interestingly, such a shock treatment is not uncommon and an analogous protocol has been studied in quantum field theory. Bouland *et al.* [48] propose that by

injecting random 1-qubit unitaries (shocks) in between time-evolutions governed by H_{CFT} (the conformal field theory Hamiltonian), one obtains a computationally pseudorandom state that is efficiently preparable. However, if the preparation protocol is not known, it requires exponentially many measurements to distinguish it from a Haar-random state. Moreover, it is unclear if such shocks scramble the initial state more than the maximally chaotic H_{CFT} . In this work, we shed more light on this and show that such shocks accelerate scrambling in quantum systems. We also go beyond and show that this noisy protocol pushes integrable systems to thermalize, which is otherwise not possible due to the presence of an extensive number of conserved quantities. Interestingly, when the noise is realized as a phase-flip channel, the recurrences that we observe in noiseless quantum circuits are strongly suppressed. As a result, the convergence toward localized Gibbs states becomes markedly smoother.

With these results, we contribute to a growing line of research that uses noise constructively in the NISQ era [49–53]. In particular, Ref. [49] proposes an algorithm that partially encodes the decoherence channels of an open quantum system and uses the intrinsic noise of quantum devices to match and simulate the full open system. This leads a reduced qubit overhead and warrants only a partial correction of residual errors. Refs. [51–53] demonstrate how nonunitary noise can be used to simulate noiseless circuits with polylogarithmic overhead in qubits and circuit depth in all-to-all connected and arbitrary architectures. Moreover, Ref. [53] mentions that unital noise irreversibly increases the entropy and pushes the complete many-body output to maximally mixed states when measured in the computational basis. In this work, we prune this argument by demonstrating that this increasing entropy accelerates the formation of localized Gibbs states as long as probed subspace is less than half the real space of the system and its complement is traced out.

These observations can be easily benchmarked by measuring all local observables in subregions of a quantum processor that span less than half the real space. Moreover, ETH guarantees that such localized Gibbs states can be prepared in all subregions of the quantum device as long as the coupling map does not completely isolate the measured qubit. Since this ascertains thermalization in localized regions, one can prepare Gibbs states using fewer resources. In addition, we show that our protocol also precludes unitary dilations [54] that are often required when simulating open systems to induce thermalization.

The rest of the paper is organized as follows: In Section II, we outline the theoretical model and the core ideas of this work. We begin in Sec. II A by describing a non-integrable extended XZ model and elaborate on the important quantities germane to this work. We further

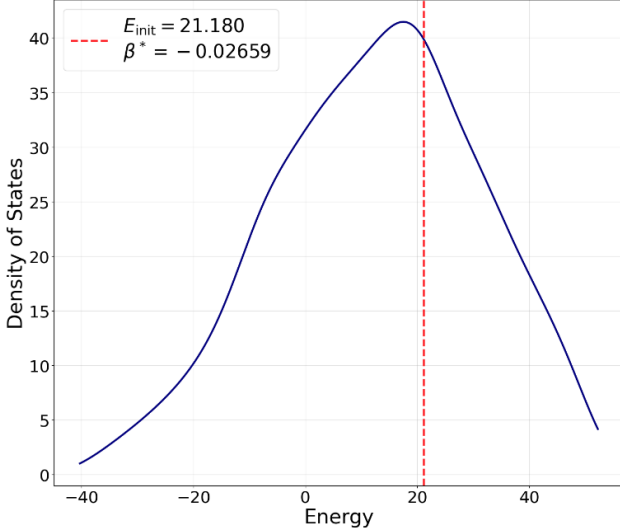


FIG. 1: **Spectrum of the Hamiltonian in Eq. (5):** We see that the spectrum is bounded on both sides. The red dotted line indicates the energy and the corresponding β^* of the arbitrarily chosen initial state. The density of states is calculated using the Kernel Density Function using a gaussian kernel and is scaled by the number of energy levels.

translate this to quantum circuits in Sec. II B and propose a noisy quantum algorithm that accelerates Gibbs state preparation. The results obtained from this setup are elaborated in Secs. III A, III B and we heuristically analyze its scaling in Sec. III C. Finally, in Sec. IV, we derive necessary conditions on the noise channel to accelerate thermalization and discuss the practical utility of our algorithm.

II. NOISE-INDUCED SCRAMBLING PARADIGM

A. Model Description and Classical Simulation

To interrogate the noise-induced accelerated thermalization protocol on NISQ devices, we consider the following spin-1/2 Hamiltonian in 1D with open boundary conditions,

$$H = -J \sum_i \sigma_i^x \sigma_{i+1}^x + J_\perp \sum_i \sigma_i^z \sigma_{i+1}^z - J' \sum_i \sigma_i^x \sigma_{i+2}^x + J'_\perp \sum_i \sigma_i^z \sigma_{i+2}^z \quad (5)$$

This describes an antiferromagnetic, extended XZ model with next-to-nearest-neighbor interactions. If the primed coefficients are identically zero, i.e., $J' = J'_\perp = 0$, the Hamiltonian becomes integrable and can be solved exactly by converting it to a system of free fermions.

This is achieved by performing a series of Jordan-Wigner and Bogoliubov transformations to convert the spin operators into spinless fermions [55]. The resulting squeezed Hamiltonian then takes the form of a 1D superconductor that can be solved exactly. By introducing next-to-nearest neighbor couplings, $J', J'_\perp \neq 0$, we make the Hamiltonian non-integrable and allow information to spread more freely through the Hilbert space. The choice of such a Hamiltonian is physically well-motivated since most quantum processors are equipped to implement at most nearest- and next-to-nearest-qubit gates [56, 57]. Moreover, cross-talk errors occurring during a quantum processor's evolution also introduce non-local couplings across the qubit architecture and further add on to the non-integrability.

To study the noise protocol in Eq. (4) on this spin chain, we consider an initial many-body product state $|\psi_0\rangle = |\uparrow\uparrow\uparrow\downarrow\cdots\downarrow\rangle$ with $|\uparrow\rangle, |\downarrow\rangle$ denoting the up and down spins respectively. Since the dimension of the full Hilbert space in this model makes exact diagonalization intractable, we work with $L = 24$ spins with $p = 3$ spins pointing up. Fig. 1 describes the spectral distribution of the Hamiltonian and the red dotted line indicates the energy of the initial state. As described in Eqs. (2), (3), the reduced density matrix $\rho_A := \text{Tr}_{\bar{A}}[|\psi_0\rangle\langle\psi_0|]$ will converge, at long times, to a thermal density matrix $\rho_A(t) = \text{Tr}_{\bar{A}}[e^{-\beta^* H}/Z]$ with vanishing corrections in the thermodynamic limit [39]. Here, β^* is defined as describing the thermal state with the average energy equal to the initial state, $\text{Tr}[He^{-\beta^* H}/Z] = \text{Tr}[H\rho_0]$. One notices that the spectrum of the Hamiltonian is bounded and allows negative values of β^* depending on the choice of the initial state. However, such a choice will not significantly affect our study, and we take the liberty to choose an arbitrary initial state agnostic to the sign of β^* .

The plain evolution of the initial state can be obtained trivially using the Schrodinger equation, $|\psi(t_{\max})\rangle = e^{-iHt_{\max}}|\psi_0\rangle$ under the Hamiltonian given in Eq. (5). To describe the noisy evolution, we break our time interval into two regions, $0 \leq t \leq t_1$ and $t_1 < t \leq t_{\max}$. In the first interval, we evolve the initial state until time t_1 . At this time, we pick three spins at random and apply a noise operator, $M_{scr}|\psi^s(t_1)\rangle$. Here, $|\psi^s(t_1)\rangle \subset |\psi(t_1)\rangle$ represents 1- and 2-spin up conserving basis states on the selected lattice sites, and M_{scr} represents a Haar random unitary that is block diagonal on 1- and 2-spin up conserving subspaces. Finally, we evolve the resultant state until t_{\max} . The plain and noisy protocols can be succinctly written as,

$$|\psi(t_{\max})\rangle = e^{-iHt_{\max}}|\psi_0\rangle \quad (6)$$

$$|\psi(t_{\max})\rangle = e^{-iH(t_{\max}-t_1)}M e^{-iHt_1}|\psi_0\rangle \quad (7)$$

Here $M|\psi(t)\rangle := M_{scr}|\psi^s(t)\rangle$ for any time t . Eq. (7) represents a simplified two-step model of the general noise protocol presented in Eq. (4). Note that while

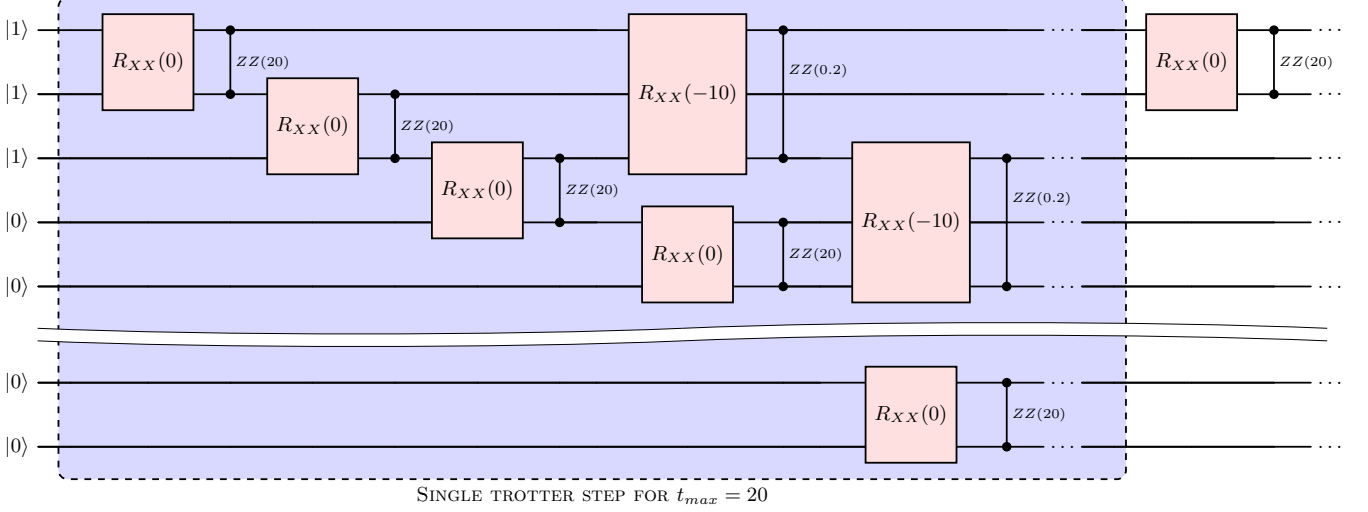


FIG. 2: Interleaved noise protocol implemented on a quantum circuit: The circuit implements the Hamiltonian (5) using noisy R_{XX} (denoted in red), and noisy R_{ZZ} gates by decomposing the time-evolution operator e^{-iHt} , under Suzuki trotterization, into gates native to the underlying architecture (here, it is decomposed into R_{XX} , and R_{ZZ} gates but the choice of gates does not change the result). Within one trotter step, each of these gates trigger a phase-flip noise with some probability and drive subsystems of a NISQ device toward a Gibbs state. For illustrative purposes, the first three qubits are initialized to $|1\rangle$. The choice of such an initial state does not significantly change the acceleration, but merely changes the target inverse temperature β of the Gibbs state the system eventually converges to.

this paradigm represents an evolution of an initial pure state, a reduced subspace of the lattice will converge to a steady state at long times. This is one of the non-trivial implications purported by ETH that we also verify numerically.

To better understand the noise application step, let the state of the system at time t_1 expressed in the spin-up conserving basis look like,

$$|\psi(t_1)\rangle = a_0(t_1) |\uparrow\uparrow\downarrow\cdots\downarrow\rangle + a_1(t_1) |\uparrow\downarrow\uparrow\cdots\downarrow\rangle + \dots + a_{2023}(t_1) |\downarrow\downarrow\cdots\uparrow\uparrow\rangle \quad (8)$$

where we work in the Schrödinger picture. Following Eq. (7), we select three sites $i, j, k \in [0, L]$, $i \neq j \neq k$ at random and apply the noise operator. This application must conserve the spin number on those sites, $\langle \sigma_i^z + \sigma_j^z + \sigma_k^z \rangle$. As the perspicacious reader would note, such an application is qubit-local, and consequently, amplitude non-local that demands multiple error-prone CNOT and Toffoli gates. To make this more physical, we design the noise operator to be block-diagonal on the 1- and 2-spin up conserving sectors, allowing us to translate the amplitude-local into qubit-local noise. Once the relevant basis states $|\psi^s(t_1)\rangle$ are identified, we apply noise by acting a Haar random unitary matrix on this subspace, $M_{scr} |\psi^s(t_1)\rangle$. This effectively shuffles their corresponding amplitudes while conserving spin-up number on those selected sites. Finally, we obtain the reduced density matrix over a test subspace of

the Hilbert space and calculate its distance from the thermal density matrix. We note that it is unclear what observables thermalize at long times according to Eq. (1). At best, ETH claims that simple observables that live in less than half the real space of the system will observe results akin to equilibrium ensembles. Since it is non-trivial to identify these observables, we analyze the behavior of a reduced density matrix as it provides an upper bound on the dynamics of the underlying observables.

Let $\rho_t = \rho(t_{\max})$ be the long-time evolved state. Then we use three distance measures, commonly employed in quantum information theory, to calculate the distance between the late-time evolved state and the thermal density matrix,

$$S_{rel}(\rho_t || \rho_{th}) = \text{Tr}[\rho_t (\ln \rho_t - \ln \rho_{th})] \quad (9)$$

$$\text{Tr}[\rho_t, \rho_{th}] = \frac{1}{2} \text{Tr} \left[\sqrt{(\rho_t - \rho_{th})^\dagger (\rho_t - \rho_{th})} \right] \quad (10)$$

$$F(\rho_t, \rho_{th}) = \left(\text{Tr} \sqrt{\sqrt{\rho_t} \rho_{th} \sqrt{\rho_t}} \right)^2 \quad (11)$$

where Eqs. (9), (10), (11) are the relative entropy, trace distance, and fidelity. In the results that follow, we employ $(1 - F(\rho_t, \rho_{th}))$, to maintain a common baseline to interpret our results. We preemptively state here that while all these distance measures describe the underlying physics equally well, we choose and show

only the ones that most accurately portray the results in the corresponding contexts.

Finally, we also study the correlation and entanglement dynamics in our system. The velocities of propagation of these pieces of quantum information are bounded by the Lieb-Robinson bound within the causal light cone and we quantify these by looking at the mutual information between the noisy and test subspaces. Let us label the noisy space, comprising the sites i, j, k as stated earlier, with N . To probe the dynamics, we look at the test subspace T and calculate,

$$I(N : T) = S_N(\rho) + S_T(\rho) - S_{NT}(\rho) \quad (12)$$

where $I(N : T)$ is the mutual information between subsystems N and T and $S_{N/T}$ is the von Neumann entropy

$$S_{N/T} = -\text{Tr}[\rho_{N/T} \ln \rho_{N/T}] \quad (13)$$

The mutual information in Eq. (12) offers a deeper understanding of the effects of noise and its role in driving the propagation of correlations across the lattice.

B. Interleaved Noise on a Quantum Circuit

To simulate the noise protocols delineated in Eqs. (4) and (7) on a quantum circuit, we implement the time-evolution operator $U(t_{max}) = e^{-iHt_{max}}$ as a unitary gate. Since the Hamiltonian in Eq. (5) consists multiple non-commuting terms, we decompose $U(t_{max})$ into Suzuki-trotterized gates and transpile them into gates native to the underlying architecture. To mimic the interleaved noise channels during unitary dynamics, we assume that noise is triggered every time a gate is implemented on the circuit. An example of such an algorithm is shown in Fig. 2 where the noisy gates are shown in red. At the end of the circuit, the initial state will have evolved till $t = t_{max}$ with noise injected during its dynamics. We show later that when these gates trigger phase-flip noise, the circuit successfully prepares localized Gibbs states at long times.

More generally, we propose that qubit-local noise that conserves $(\langle \sigma_{i_1}^z \sigma_{i_2}^z \dots \sigma_{i_N}^z \rangle + \mathbb{I})/2$, where N denotes the number of noisy qubits, will accelerate Gibbs state preparation. In the Pauli noise model, this channel is written as,

$$M[\rho] := M\rho M^\dagger = \sum_l p_l P_l^{(m)} \rho P_l^{(m)} \quad (14)$$

where $P_l^{(m)}$ is a Pauli string with support on m qubits. Under the aforementioned noise constraints, an $m = 2$ -qubit local Pauli string admits elements,

$P_l^{(2)} \in \left\{ \sigma_i^z \sigma_j^z, \sigma_i^x \sigma_j^x \frac{\mathbb{I} - \sigma_i^z \sigma_j^z}{2}, \mathbb{I} \right\}$. We see that this reduces to a phase-flip channel for $p_0 = p, p_1 = 0, p_2 = (1 - p)$, and the Haar-random unitary channel when the distribution of the probabilities are Haar-random under unitary constraints.

In Sec. IV, we implement this algorithm by applying noisy 1- and 2-qubit gates under the phase-flip noise channel and look at the convergence toward Gibbs states in $T \neq N$.

C. Thermalization of integrable systems

In general, integrable systems are known to not thermalize at long times due to the presence of an extensive number of conserved quantities. These quantities limit the propagation of initial information to small subspaces of the total Hilbert space. A simple example of such an integrable system is one with non-interacting spins. However, we propose that by introducing noise, we momentarily increase the range of couplings, introduce non-integrability, and allow information to freely flow in the Hilbert space. Using this paradigm, integrable systems can be made non-integrable, and certain degrees of freedom can be allowed to obey ETH to eventually thermalize at long times. In Sec. IV, we analyze this behavior and discuss the results.

III. RESULTS

A. Classical Simulation

Following the theory outlined in Section II A, we investigate the plain and noisy dynamics of the initial product state, where the first three spins point up, governed by the Hamiltonian in Eq. (5). In Fig. 3a, the solid and dotted lines denote the noisy and plain dynamics respectively. The time domain is discretized into 50 equal intervals where noise is applied as a shock at the 2nd timestep. This can be verified by observing that both lines coincide leading to this point, after which they diverge. We observe the test subspace, $T \in [L, L-1, L-2]$, of the density matrix and obtain its distance from the thermal state using suitable distance measures. We see that the shock accelerates the thermalization process as evidenced by (i) higher decay rate as shown in the inset, and (ii) sustained closeness of solid lines vs dotted lines at long times. We also see that the energy of the final state does not fluctuate, indicating that the initial state converges to the appropriate thermal state. We fit the trace distance curves with an exponentially decaying function and find the decay rates to be $\kappa_{plain} \approx 0.443, \kappa_{noisy} \approx 1.187$. These can readily be verified by calculating the slopes

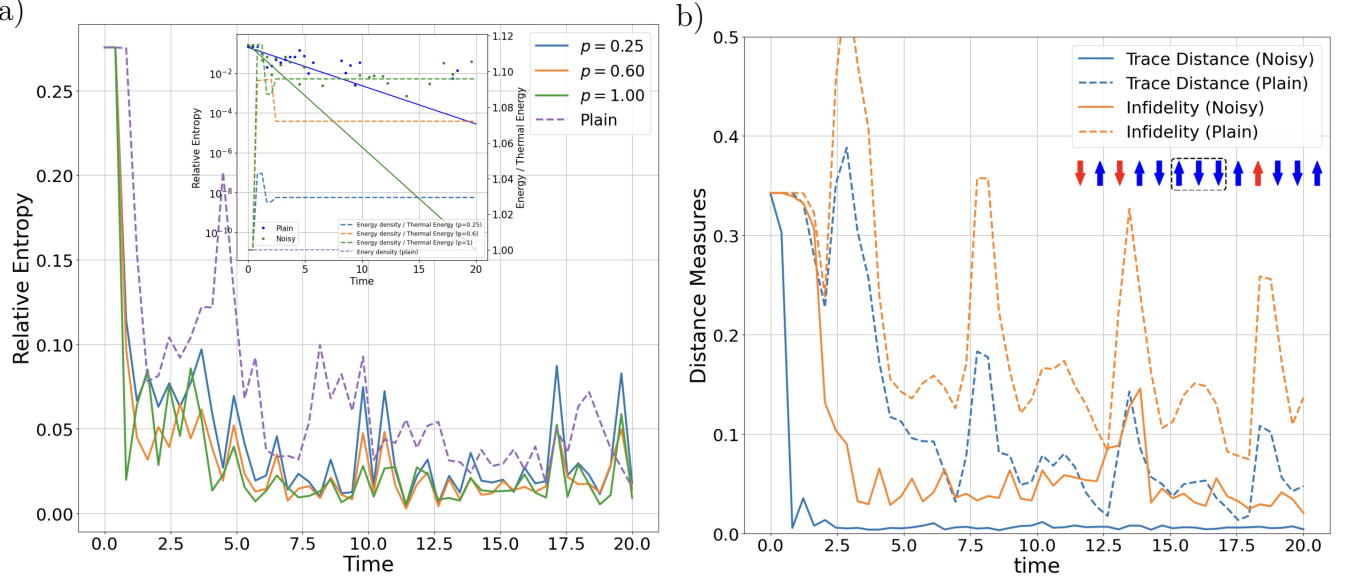


FIG. 3: **Comparison between noisy and plain evolutions toward a Gibbs state:** In (a) we study the relative entropy between the noisy evolution (solid) and the Gibbs state, and compare the same with that of the plain evolution (dotted) with the same Gibbs state. We see that the both the evolutions overlap in the beginning and diverge once the noise is applied. The former accelerates thermalization as witnessed by (i) higher decay rate as shown in the inset, and (ii) sustained closeness of solid lines vs dotted lines, and sustained energy of the state at long times. In (b) we look at the ability of noise to introduce non-integrability in an integrable system and aid thermalization. The dotted lines observe recurrences during its evolution and indicate that the system does not thermalize. However, the solid lines observe a sustained decay and converge to a thermal state. The insets depict a condensed representation of the spin chain, where three noisy spins are highlighted in red. The configurations shown correspond to two randomly selected examples for illustrative purposes.

of the curves given in insets of Fig. 3a, where the green (noisy) curve decays faster than the blue (plain) curve. The dotted lines shown in the same inset tracks the ratio of the energy density with the thermal energy. Since the spectrum of the Hamiltonian is bounded and the inverse temperature β is negative for our choice of initial state, we measure the energy densities with respect to the highest energy state, $\text{Tr}(He^{-\beta H}/Z)$ for traceless H and $\beta \rightarrow -\infty$. From the blue, orange, and green dotted curves, we see that noise pushes the state toward lower energy and, consequently, higher density of states, $\text{DOS} = e^S$ to leading order in the system size. If the microcanonical entropy S tracks T , then these correspond to states of highest entropy that are indicative of thermal distributions.

While we showed that noise accelerates thermalization in non-integrable systems, it is curious to see if it can momentarily introduce non-integrability and induce thermalization in integrable systems. In Fig. 3b, we reduce $J'_\perp = J' = 0$ and see that the dotted lines representing plain dynamics oscillate rapidly and do not thermalize. However, these oscillations become subdued in the noisy protocol and lead to thermalization at long times. For the sake of clarity, we do not show the relative entropy but find it to replicate the dynamics of

other distance measures equally well. The inset shows a representation of a 1D spin chain where the red denotes noisy spins and the box represents the test subspace, T .

Having discussed the role of noise in accelerating the convergence to Gibbs states, it is imperative to juxtapose the implications of our protocol with other types of noise occurring during Hamiltonian simulations. For example, we compare the Haar-random unitary noise with the phase-flip channel. This channel is modeled as,

$$\mathcal{E}(\rho) = (1-p)\rho + pS^z\rho S^z \quad (15)$$

where $S_z = \sigma_i^z \sigma_j^z \sigma_k^z$, $i \neq j \neq k \in N$. Note that this is a 3-qubit phase flip operation and does not contain single-qubit operations like $\mathbb{I}_i \sigma_j^z \mathbb{I}_k$. For the purposes of our study, we compare with the 3-qubit operation but note that it can be readily generalized to other sectors. This noise channel is an effective discrete-time mapping of microscopic dephasing processes occurring in continuous time. This includes photons traveling along a waveguide, electronic states feeling the effects of distant charges [58], etc. In Fig. 4, we see that the phase flip noise also successfully accelerates thermalization dynamics. This is reinforced in the inset where the corresponding values of the decay rates, κ , lie very close

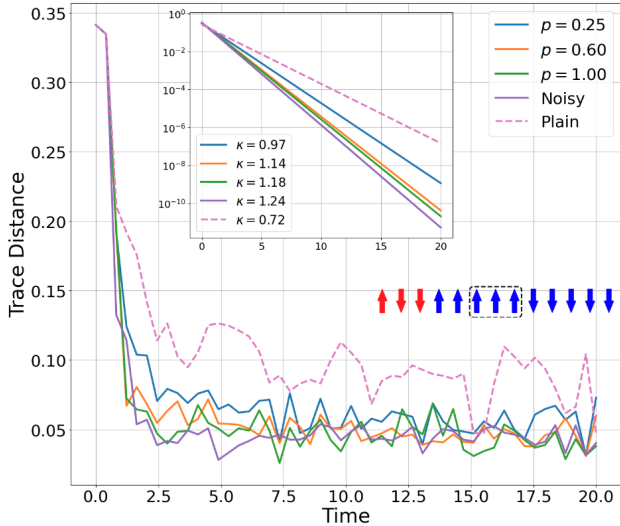


FIG. 4: Phase-flip noise vs Haar random unitary noise: The main plot shows that the trace distances decay at the same rate for both phase-flip noises at all probabilities and the Haar-random unitary noise. This is reinforced in the inset where the corresponding values of κ lie very close to each other but are higher than the plain-evolved dynamics. The second inset illustrates a condensed lattice of spins with red spin denoting the noisy space and the dotted box describes the test space.

to each other and are higher than the decay rate of the plain-evolved dynamics. This informs us that naturally occurring phase-flip errors are sufficient to efficiently prepare localized Gibbs states in a laboratory. More generally, this hints to a pattern where any quantum channel that changes the superposition of the basis states and takes the system to higher entropy will accelerate it to a Gibbs state. Such a channel is described by the noise model in Eq. (14).

Two questions arise at this point: (i) What determines the timescale of thermalization in the system?; and (ii) How does the rate of noise-induced accelerated thermalization vary across different regions of the system? We note that for subsystems to thermalize, information must propagate from the initial subspace I to a test subspace T . This implies that the velocity of entanglement propagation from I to T sets a lower bound on the timescale for thermalization of T . From earlier discussions, we infer that noise acting on any N accelerates thermalization time scales, and consequently, must increase the velocity of entanglement propagation. To understand how this effect of noise impacts thermalization timescales across the system, we look at the growth of mutual information between N and T . This is because it encapsulates the growth of correlations between N and T and directly gives information about the impact of the noise. We show in Fig. 5 that such an analysis reveals regimes where correlations grow faster

than others. Studying such velocities is also common across various areas of physics, where the moniker, "tsunami velocity" [59] is also used. In many models of interest to high-energy physics, this can be calculated analytically using holographic techniques [60]. The Lieb-Robinson (LR) bound sets an upper limit on such a rate of growth of information in non-relativistic systems [61], and guides our study on the effects of noise across the lattice.

In Fig. 5a, we examine the growth of correlations by calculating the mutual information between the test subspace $T \in [L/2 - 1, L/2, L/2 + 1]$ and the noisy sites, N as indicated in the legend. By comparing the solid and dotted curves, we readily see that noise-induced correlations grow faster than those due to coherent transport under the Hamiltonian. These correlations eventually plateau when the subsystem thermalizes. We also see that the solid lines observe an early onset of the plateau and eventually converge with the coherent dynamics at long times. Since the two noisy spaces, N_1, N_2 shown in violet in both the insets, are equally spaced from T (dotted box), we do not see an appreciable difference in their correlation dynamics. However, this is violated in Fig. 5b where $T \in [0, 1, 2]$ and N_1, N_2 are unequally spaced from it. The red lines show an early onset of growth in mutual information and indicate that the correlations from $N_1 \in [L/4, L/4 - 1, L/4 + 1]$ reach T faster than the correlations from $N_2 \in [L - 1, L - 2, L - 3]$. Such a behavior concurs with the finite velocity of information propagation bounded by the LR velocity. Interestingly, if N and T overlap, we see a rapid growth in mutual information, as witnessed by the early rise in the red curves in Fig. 5c. Here $T \in [L/2, L/2 - 1, L/2 + 1]$ and overlaps with $N_2 \in [0, L/2, L - 1]$ on site $L/2$. This is likely because the noise applied in the overlapping subspace immediately contributes to the growth of correlations in the same space. More notably, we see a large difference in the plateaus of mutual information from overlapping (red) and non-overlapping (blue) noise sites that hints that the shock-induced correlations spread non-uniformly throughout the lattice.

The early onsets of growth outlined in these paragraphs arise due to the differing distances between N and T , where the velocities are likely preserved. However, this does not capture the entire picture. In Fig. 5d, we fix the distance between N and T , apply a cascade of shocks, and investigate the early onset as a function of frequency of noise applications. We calculate the velocity of propagation of correlations by fitting the curves and extracting the rate. The fitted curves tell us that increasing noise applications do not bring a significant change in the correlation propagation velocity. This is likely because a non-integrable system thermalizes by itself under noiseless evolution, and a single Haar-random unitary readily saturates its bound. As a result, further applications pale any observable effects. These curves

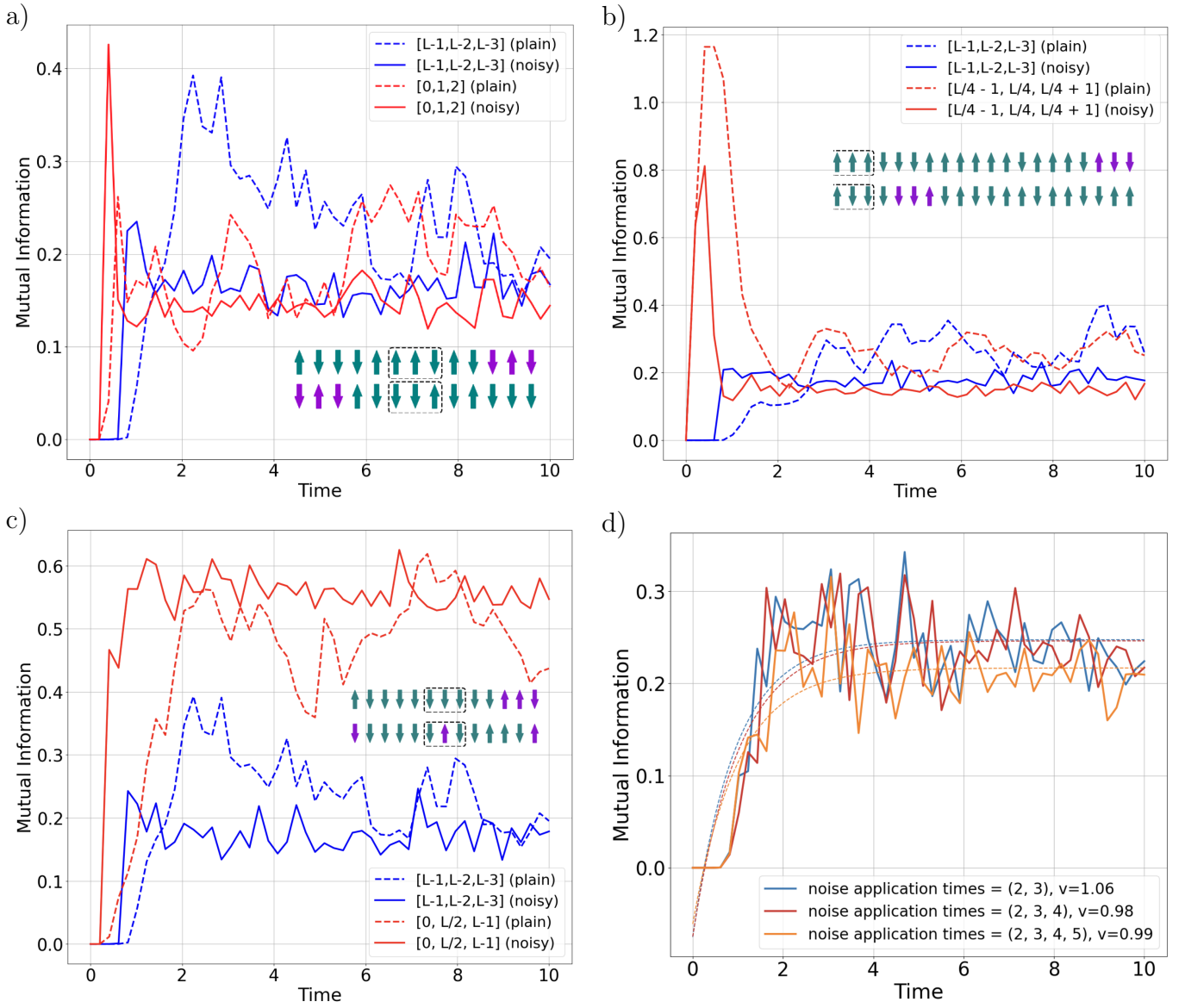


FIG. 5: Growth of mutual information in noiseless and noisy protocols: (a) Shows the dynamics of correlations of noise subspaces (violet spins) $N_1 \in [L-1, L-2, L-3]$, $N_2 \in [0, 1, 2]$ placed at equal distances from the test subspace, T (dotted). We see that the noise accelerates correlation propagation as compared to that due to coherent transport (violet spins replaced with green spins). The initial sharp rise of the red line is likely due to the overlap of N_1 with the initial state. (b) Dynamics of correlations of noise applied at unequal distances with $T \in [0, 1, 2]$. We see the correlations from $N_1 \in [L/4 - 1, L/4, L/4 + 1]$ reach T earlier than from $N_2 \in [L-1, L-2, L-3]$ and observe a larger increase in the mutual information. (c) A part of N , T overlap and we see a faster growth in correlations and greater plateau of correlations from the overlapping space. Finally, in (d) we apply a cascade of shocks on $N \in [L-1, L-2, L-3]$ and observe that the velocity of information propagation to $T \in [0, 1, 2]$ does not change significantly. This is likely because a non-integrable system thermalizes by itself and consequently, a single noise application readily saturates the bound on velocity.

eventually plateau around the same range of values and indicate the convergence to the same thermal state using different noise paradigms. While a single shock saturates the rate of thermalization of non-integrable systems, we will see later that a cascade of shocks further

enhances the rate of thermalization of integrable systems.

It is noteworthy to mention that the study above was conducted by modeling qubits as spins on a one dimensional lattice. These results also hold if the degrees of free-

dom are modeled as hardcore bosons or as fermions on a one-dimensional lattice with their corresponding non-integrable Hamiltonians. While we do not discuss these systems here, its source code and results can be found as part of the repository for this work.

B. Quantum Simulation

The classical simulation results obtained above must also translate well in the complete 2^L computational basis of a NISQ device since the corrections to ETH become vanishing in the thermodynamic limit. Here, we consider a 12 qubit quantum computer implementing the Hamiltonian in Fig. (5). To implement the noise model described in Eq. (14) and interleave it in between unitary dynamics as in Eq. (4), we assume that noise is triggered each time a gate is implemented on a quantum circuit as shown in Fig. 2. Performing a similar analysis, we see in Fig. 6 that the distance measures obtained using a noiseless quantum circuit (described by dotted lines) observes multiple recurrences while converging to a Gibbs state. However, when these gate implementations trigger a phase-flip noise, they suppress the recurrences, introduce non-integrability, and drive the system smoothly towards a Gibbs state.

One sees that these results appear to be more pronounced in quantum circuits than in classical simulations of Fig. 3a. This is likely due to the multiple noisy gate implementations arising from higher-order trotterization. These effectively trigger a cascade of shocks, overcome trotter errors, and smoothly suppress all the recurrences.

C. Heuristic Scaling

In this section, we heuristically study the time complexity of our quantum channel by measuring the decay rate to solution. To do this, we fit an exponential function to the distance measures shown earlier and obtain its decay rate κ_{th} . In a similar manner, we fit both the noisy and plain dynamics and obtain the quantity, $\kappa_{th}^{\text{noisy}}/\kappa_{th}^{\text{plain}}$ that captures the advantage of our noisy quantum channel to accelerate thermalization.

First, we look at how the quantity $\kappa_{th}^{\text{noisy}}/\kappa_{th}^{\text{plain}}$ scales with the frequency of noise applications. In Fig. 7, we look at an integrable model by reducing $J' = J'_\perp = 0$ from Eq. (5) and vary the coefficient of the Ising term J_\perp . Curiously, a single application of noise fails to overcome integrability in weakly interacting regimes since $\kappa_{th}^{\text{noisy}}/\kappa_{th}^{\text{plain}} \approx 1$. It is only at $J_\perp \approx 1.0$ that we observe a more appreciable advantage, suggesting the presence of a threshold beyond which the noise becomes effective in thermalizing integrable systems. By further applying noise, we see that our protocol improves in its ability to accelerate the preparation of

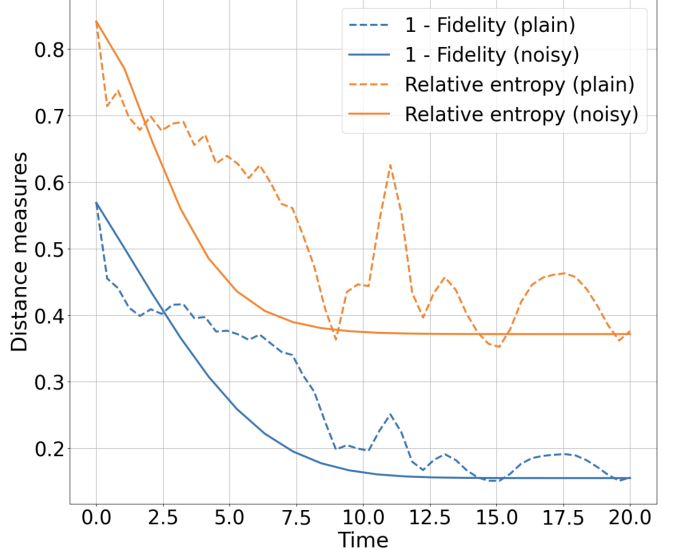


FIG. 6: **Thermalization of a subspace of a noisy quantum circuit under phase-flip noise:** Noise is triggered whenever a gate is implemented on the quantum circuit. We observe that the phase-flip channel suppresses the recurrences and enables smoother convergence to localized Gibbs states.

Gibbs states. This is also reinforced in Fig. 6 where the circuit involves the decomposition of the Hamiltonian into multiple noisy gates. These gates trigger multiple instances of noise and pushes the system to smoothly decay into a Gibbs state. From the inset in Fig. 7, we see that for non-integrable Hamiltonians, the advantage saturates for a much lower number of noise applications than that of the integrable model. This is expected since a non-integrable model is known to thermalize by itself and fewer applications of noise suffice in thermalization. However, for an integrable model, we see that a cascade of shocks further enhances the rates of thermalization up to a factor of $\sim 4.5x$. The scaling of the advantage appears to be logarithmic in the frequency of noise applications.

While our quantum circuit from Fig. 2 models at most two-qubit noise, NISQ devices may also incur cross-talk errors among multiple qubits, often located at distant locations in real space. It is thus imperative to understand the thermalization dynamics as a function of the number of sites the noise acts on. In Fig. 8, we see that increasing the number of noisy sites leaves the dynamics invariant, suggesting that the effects of noise delocalize throughout the lattice faster than the increasing size of the initial noisy sites propagating an appreciable influence. As a result, Gibbs states can be prepared efficiently by allowing noise to act on an arbitrary number of qubits.

Finally, we study the scaling of our protocol with respect to the system size L . In fig. 9, we see that the rate of

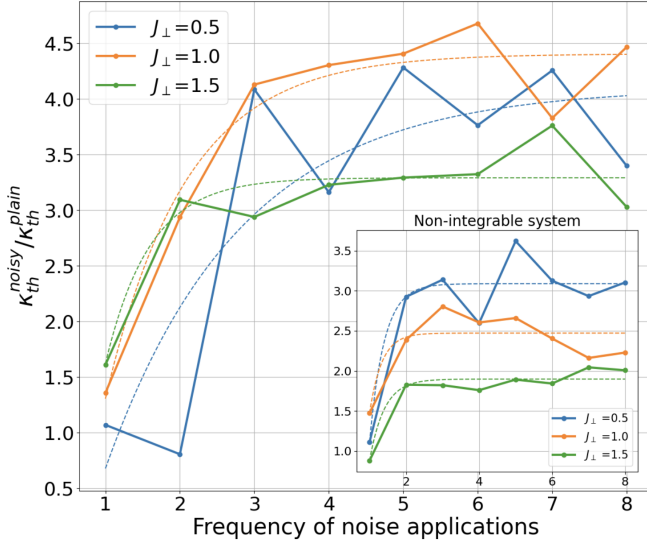


FIG. 7: Scaling of the ratio of the thermal decay rates as a function of the frequency of noise applications: We see that the quantity $\kappa_{th}^{noisy}/\kappa_{th}^{plain}$ scales logarithmically with the increasing the applications of noise. This holds equally well for both integrable and non-integrable (inset) Hamiltonians. In fact, the acceleration is more pronounced in the former while both saturate at higher frequencies. Here, $T \in [L, L-1, L-2]$ and N is chosen arbitrarily.

decay nearly triples as we scale the system to 30 sites (dim = 4060). Similarly, as we scale the quantum circuit 12 physical qubits (dim = 4096), we see from the inset that the dynamics do not offer a significant difference. This is likely because the multiple noisy gate applications saturate the acceleration leaving no room for additional advantage in an otherwise non-thermalizing system (dotted lines).

IV. DISCUSSION

A. Why does this work?

In this section, we elucidate the necessary conditions on the noise operator, M , to accelerate thermalization. As stated earlier, consider the plain evolution of an initial density matrix ρ_0 as,

$$\rho(t_{max}) = e^{-iHt_{max}} \rho_0 e^{iHt_{max}} \quad (16)$$

where H is given by Eq. (5). We implement the noise model similar to Eq. (16) but intersperse it with the operator M at arbitrary intervals in time $0 \leq t \leq t_{max}$ as given in Eq. (4). For simplicity, let us consider a two-step noise model as,

$$\rho'(t_{max}) = \mathcal{N}^{(1)} \cdot \rho_0 \cdot \mathcal{N}^{\dagger(1)} \quad (17)$$

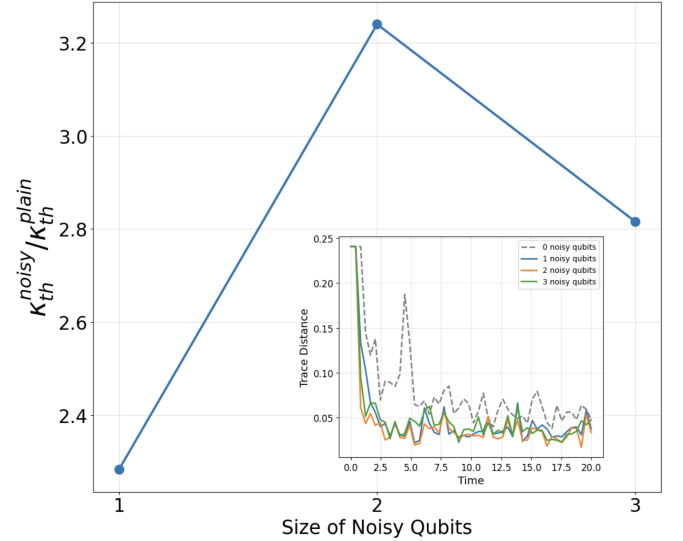


FIG. 8: Scaling of the ratio of decay rates to a Gibbs state as a function of the number of noisy sites: We see that increasing the size does not uniformly scale the advantage, suggesting little observable difference. This is reinforced in the inset where the decay of the trace distances are nearly identical for different noisy qubits. Here, $T \in [L, L-1, L-2]$ and N is chosen arbitrarily.

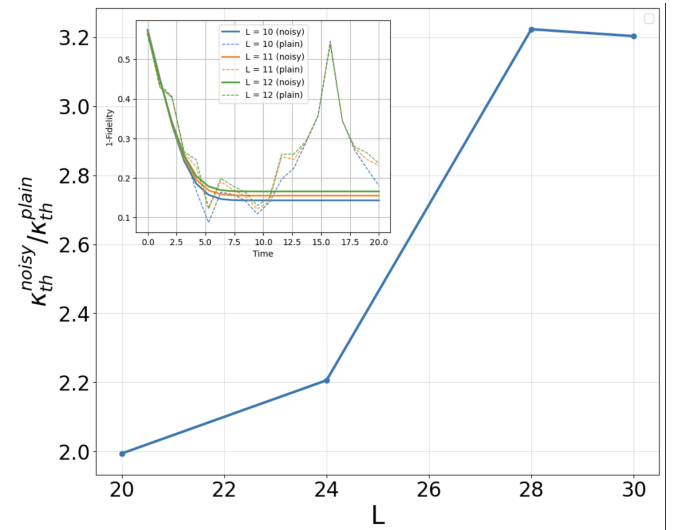


FIG. 9: Scaling of $\kappa_{th}^{noisy}/\kappa_{th}^{plain}$ with the dimension of Hilbert space (number of qubits): We see that this quantity scales linearly with the size of the underlying lattice. On a quantum circuit, the numerous noise gates saturate the acceleration (inset) and leave little room for additional advantage. Here, $T \in [L, L-1, L-2]$ and N is chosen arbitrarily.

where $\mathcal{N}^{(1)} = e^{-iH(t_2-t_1)}Me^{-iHt_1}$. As before, we partition the real space into two subspaces, A and B . Without loss of generality, we assume that M is applied on subsystem B , and we look at the propagation of correlations to subsystem A . The final state reduced density matrices over this subspace for the noiseless and noisy protocols are defined as,

$$\rho_A(t_2) = \text{Tr}_B[e^{-iHt_2}\rho_0e^{iHt_2}] \quad (18)$$

$$\rho'_A(t_2) = \text{Tr}_B[e^{-iH(t_2-t_1)}M\rho(t_1)M^\dagger e^{iH(t_2-t_1)}] \quad (19)$$

From Eqs. (18), (19), we see that if $[M, H] \neq 0$, then $\rho'_A(t) \neq \rho_A(t)$ and the noisy protocol produces a different final state. This condition generally holds true since the set of thermalizing noise operators is very large and most noise operators fail to commute with H . However, in special cases where M is a symmetry, i.e. $[M, H] = 0$, the protocol still produces a different state if M straddles the boundary between A and B . In this case, it is not cyclic under the trace in Eq. (19) and $\rho'_A(t) \neq \rho_A(t)$.

Now, let us consider the Hilbert-Schmidt norm of the difference between these final states and the infinite temperature state,

$$\|\rho'_A(t) - \rho_A^\infty\|_2 = \text{Tr}[\rho'_A(t)^2] - \frac{1}{d_A} \quad (20)$$

$$\|\rho_A(t) - \rho_A^\infty\|_2 = \text{Tr}[\rho_A(t)^2] - \frac{1}{d_A} \quad (21)$$

where $\|\cdot\|_2$ is the Hilbert-Schmidt norm. To characterize the growth of entanglement between the two subsystems, we look at the α -Rényi entropy defined as $S_\alpha = \frac{1}{1-\alpha} \ln(\text{Tr}[\rho^\alpha])$. For $\alpha = 2$, we can then write $\text{Tr}[\rho^2] = e^{-S_2}$ and note that the purity of the reduced subsystem is inversely proportional to its Rényi-2 entropy. Popescu *et al.* [45] argue that any typical state will comprise subsystems that are maximally entangled with the rest of the system. Since M is shown to produce a state, $\rho'_A(t)$ different from $\rho_A(t)$, it forms a typical state. As a result, we conclude that the operator M necessarily increases the entanglement between subsystems A and B . This increases the Rényi-2 entropy in the noisy protocol and consequently results in the inequality,

$$\|\rho'_A(t) - \rho_A^\infty\|_2 \leq \|\rho_A(t) - \rho_A^\infty\|_2 \quad (22)$$

Since any quantum channel that increases entanglement between two subsystems gets them closer to the thermal state, we conclude that $\rho'_A(t)$ is closer to the thermal state than $\rho_A(t)$. These arguments elucidate the likelihood of a perturbation to nudge a state towards higher entropy and lead to the appropriate thermal state. The inset in Fig. 3a numerically demonstrates these arguments within statistical fluctuations. Finally, we observe

that our proposed noise model in Eq. (14) does not commute with the Hamiltonian in Eq. (5) and thus satisfies the aforementioned conditions.

B. Practical Utility

The ETH-based noise algorithm that we propose in this work can be easily tested on experiments with quantum computers. More specifically, one can pick a small region in a quantum processor and measure all local observables in those regions. ETH guarantees that the results of these measurements converge to the thermal expectation values corresponding to the appropriate inverse temperature, as long as the selected region spans lesser than half the real space of the system. Using the algorithm we propose in Eqs. (4), (14), one can then benchmark the timescales of these measurements with varying rates of noise. Interestingly, since these rates (such as the T_2 noise rate) vary rapidly on a daily basis, one must be able to systematically observe the advantage proposed using a wide sample size of noise.

In addition to the timescale advantage, ETH also guarantees that every subregion in the quantum processor hosts thermally expected values of observables as long as the probed region spans less than half the real space. This allows experimental flexibility to observe Gibbs states in multiple regions and precludes one from explicitly preparing these states in select regions. Moreover, the locality of these states offers one to prepare them using fewer resources. Since this protocol does not require unitary dilations [54] to simulate open system, it also offers the advantage to prepare these states with reduced overhead in ancilla qubits.

Since a rigorous mechanism for the emergence of these localized Gibbs states is not well-understood, it is non-trivial to analytically explore the advantage. However, one can easily perform relevant measurements on a noisy quantum processor and certify the advantages we reveal in this work. Finally, we note that since ETH is agnostic to the underlying architecture of a NISQ device, our protocol is versatile across all modalities and coupling maps subject to the constraints presented in this work.

V. SUMMARY AND OUTLOOK

In this work, we propose a protocol to use noise to accelerate the preparation of Gibbs states in the current NISQ era of quantum computation. By deriving ideas from the Eigenstate Thermalization Hypothesis, we show that when noise is interleaved between unitary dynamics of a quantum circuit, it momentarily introduces non-integrability, enhances chaotic dynamics and accelerates the preparation of localized Gibbs states by up to a factor of $\sim 3.5x$ compared to noiseless systems.

Interestingly, we find that the naturally occurring phase-flip noise is sufficient in realizing this advantage. To demonstrate these results, we (i) classically simulate our noisy protocol on a 1D spin-1/2 chain governed by an extended XZ model and (ii) replicate it on a quantum circuit each gate triggers a phase-flip channel. In both cases, we see that noise not only accelerates the convergence to localized Gibbs states, but also induces thermalization in integrable Hamiltonians and quantum circuits, where the former otherwise fails due to an presence of extensive number of conserved quantities.

We further analyze the mechanism behind this acceleration by studying the growth of mutual information between noisy qubits and an arbitrarily chosen test spins. Comparing these dynamics with and without noise, we find that noise increases the effective velocity of information propagation, enabling subsystems to reach their steady states earlier than they would in coherent evolution alone. In addition, we observe that the convergence to Gibbs states scales logarithmically with the frequency of noise applications in both integrable and non-integrable regimes, with the effect being more pronounced in the former where plain evolution does not lead to thermalization. In the absence of trotterization, we see that the rate of thermalization scales linearly with the system size.

Finally, we analytically show that the noise operator can

provide these advantages only if it is (i) sufficiently non-local and (ii) does not commute with the Hamiltonian. Taken together, this work delineates a regime where noise can be harnessed as a resource in the quantum computing pipeline and help derive quantum advantage before the advent of fully fault-tolerant quantum computers.

DATA AVAILABILITY

The data that support the findings of this article can be obtained from the authors upon reasonable request.

ACKNOWLEDGMENTS

We thank Lukasz Cincio, Marco Cerezo, and Nai-Hui Chia for useful discussions. SD also thanks Los Alamos National Laboratory for support during different stages of this project. PH was supported by the National Science Foundation grant no. DMR 20471943. ERB and SD were supported by National Science Foundation under CHE-2404788 and the Robert A. Welch Foundation (E-1337). Y.Z. acknowledges the support from Laboratory Directed Research and Development (LDRD) program of Los Alamos National Laboratory (LANL). LANL is operated by Triad National Security, LLC, for the National Nuclear Security Administration of the U.S. Department of Energy (contract no. 89233218CNA000001).

[1] A. M. Childs, D. Maslov, Y. Nam, N. J. Ross, and Y. Su, *Proceedings of the National Academy of Sciences* **115**, 9456 (2018).

[2] R. P. Feynman, in *Feynman and computation* (cRc Press, 2018) pp. 133–153.

[3] N. Gisin and R. Thew, *Nature photonics* **1**, 165 (2007).

[4] C. L. Degen, F. Reinhard, and P. Cappellaro, *Reviews of modern physics* **89**, 035002 (2017).

[5] N. Gisin, G. Ribordy, W. Tittel, and H. Zbinden, *Reviews of modern physics* **74**, 145 (2002).

[6] L. Huynh, J. Hong, A. Mian, H. Suzuki, Y. Wu, and S. Camtepe, arXiv preprint arXiv:2308.11269 (2023).

[7] J. Biamonte, P. Wittek, N. Pancotti, P. Rebentrost, N. Wiebe, and S. Lloyd, *Nature* **549**, 195 (2017).

[8] S. B. Ramezani, A. Sommers, H. K. Manchukonda, S. Rahimi, and A. Amirlatifi, in *2020 International joint conference on neural networks (IJCNN)* (IEEE, 2020) pp. 1–8.

[9] F. G. Brandao and K. M. Svore, in *2017 IEEE 58th Annual Symposium on Foundations of Computer Science (FOCS)* (IEEE, 2017) pp. 415–426.

[10] R. D. Somma, S. Boixo, H. Barnum, and E. Knill, *Physical review letters* **101**, 130504 (2008).

[11] Z. Lu and O. Raz, *Proceedings of the National Academy of Sciences* **114**, 5083 (2017).

[12] P. Brooks and J. Preskill, *Physical Review A—Atomic, Molecular, and Optical Physics* **87**, 032310 (2013).

[13] E. T. Campbell, B. M. Terhal, and C. Vuillot, *Nature* **549**, 172 (2017).

[14] T. Albash, V. Martin-Mayor, and I. Hen, *Physical review letters* **119**, 110502 (2017).

[15] S. Vinjanampathy and J. Anders, *Contemporary Physics* **57**, 545 (2016).

[16] S. Deffner and S. Campbell, *Quantum Thermodynamics: An introduction to the thermodynamics of quantum information* (Morgan & Claypool Publishers, 2019).

[17] D. Poulin and P. Wocjan, *Physical review letters* **103**, 220502 (2009).

[18] M.-H. Yung and A. Aspuru-Guzik, *Proceedings of the National Academy of Sciences* **109**, 754 (2012).

[19] A. Riera, C. Gogolin, and J. Eisert, *Physical review letters* **108**, 080402 (2012).

[20] D. B. Kaplan, N. Klco, and A. Roggero, arXiv preprint arXiv:1709.08250 (2017).

[21] M. Motta, C. Sun, A. T. Tan, M. J. O’Rourke, E. Ye, A. J. Minnich, F. G. Brandao, and G. K.-L. Chan, *Nature Physics* **16**, 205 (2020).

[22] Y. Wang, G. Li, and X. Wang, *Physical Review Applied* **16**, 054035 (2021).

[23] X.-Y. Guo, S.-S. Li, X. Xiao, Z.-C. Xiang, Z.-Y. Ge, H.-K. Li, P.-T. Song, Y. Peng, Z. Wang, K. Xu, *et al.*, *Chinese Physics B* **32**, 010307 (2023).

[24] G. Verdon, J. Marks, S. Nanda, S. Leichenauer, and J. Hidary, arXiv preprint arXiv:1910.02071 (2019).

- [25] A. N. Chowdhury and R. D. Somma, arXiv preprint arXiv:1603.02940 (2016).
- [26] M. E. Edo and L.-A. Wu, arXiv preprint arXiv:2403.14630 (2024).
- [27] D. Aharonov, I. Arad, and T. Vidick, *Acm sigact news* **44**, 47 (2013).
- [28] S. Sgroi, S. Lorenzo, L. Innocenti, P. A. Erdman, G. M. Palma, and M. Paternostro, arXiv preprint arXiv:2506.20625 (2025).
- [29] T. E. Baker, arXiv preprint arXiv:2504.19185 (2025).
- [30] P. Reimann, *Nature communications* **7**, 10821 (2016).
- [31] L. Coopmans, Y. Kikuchi, and M. Benedetti, *PRX Quantum* **4**, 010305 (2023).
- [32] H. Perrin, T. Scoquart, A. I. Pavlov, and N. V. Gnezdilov, *Communications Physics* **8**, 95 (2025).
- [33] D. A. Lidar and T. A. Brun, *Quantum error correction* (Cambridge university press, 2013).
- [34] Z. Cai, R. Babbush, S. C. Benjamin, S. Endo, W. J. Huggins, Y. Li, J. R. McClean, and T. E. O'Brien, *Reviews of Modern Physics* **95**, 045005 (2023).
- [35] S. Endo, S. C. Benjamin, and Y. Li, *Physical Review X* **8**, 031027 (2018).
- [36] L. Viola, E. Knill, and S. Lloyd, *Physical Review Letters* **82**, 2417 (1999).
- [37] K. Khodjasteh and D. A. Lidar, *Physical review letters* **95**, 180501 (2005).
- [38] R. Pathria and P. D. Beale, *5 - Formulation of quantum statistics, Editor(s): R.K. Pathria, Paul D. Beale, Statistical Mechanics (Fourth Edition), Pages 117-154* (Academic Press, 2022).
- [39] J. R. Garrison and T. Grover, *Physical Review X* **8**, 021026 (2018).
- [40] J. M. Deutsch, *New Journal of Physics* **12**, 075021 (2010).
- [41] J. M. Deutsch, *Physical review a* **43**, 2046 (1991).
- [42] M. Srednicki, *Physical review e* **50**, 888 (1994).
- [43] M. Srednicki, *Journal of Physics A: Mathematical and General* **32**, 1163 (1999).
- [44] S. Goldstein, J. L. Lebowitz, R. Tumulka, and N. Zanghì, *Physical review letters* **96**, 050403 (2006).
- [45] S. Popescu, A. J. Short, and A. Winter, *Nature Physics* **2**, 754 (2006).
- [46] C. Murthy and M. Srednicki, *Physical Review E* **100**, 022131 (2019).
- [47] T.-C. Lu and T. Grover, *Physical Review E* **99**, 032111 (2019).
- [48] A. Bouland, B. Fefferman, and U. Vazirani, arXiv preprint arXiv:1910.14646 (2019).
- [49] S. Dambal, A. Sone, and Y. Zhang, arXiv preprint arXiv:2510.21075 (2025).
- [50] P. M. Harrington, E. J. Mueller, and K. W. Murch, *Nature Reviews Physics* **4**, 660 (2022).
- [51] T. Schuster, C. Yin, X. Gao, and N. Y. Yao, *Physical Review X* **15**, 041018 (2025).
- [52] M. Ben-Or, D. Gottesman, and A. Hassidim, arXiv preprint arXiv:1301.1995 (2013).
- [53] O. Shtanko and K. Sharma, *PRX Quantum* **6**, 030347 (2025).
- [54] A. W. Schlimgen, K. Head-Marsden, L. M. Sager, P. Narang, and D. A. Mazziotti, *Physical Review Letters* **127**, 270503 (2021).
- [55] H. Cheraghi and S. Mahdavifar, *Scientific Reports* **10**, 4407 (2020).
- [56] S. Chatterjee, B. K. Behera, and F. J. Seo, *Applied Sciences* **13**, 12075 (2023).
- [57] C. Zhang, Z. Guan, Y. Qian, and S. Feng, in *2022 International Conference on Computing, Communication, Perception and Quantum Technology (CCPQT)* (IEEE, 2022) pp. 402–409.
- [58] M. A. Nielsen and I. L. Chuang, *Quantum computation and quantum information* (Cambridge university press, 2010).
- [59] H. Casini, H. Liu, and M. Mezei, *Journal of High Energy Physics* **2016**, 1 (2016).
- [60] H. Liu and S. J. Suh, *Physical review letters* **112**, 011601 (2014).
- [61] S. Bravyi, M. B. Hastings, and F. Verstraete, *Physical review letters* **97**, 050401 (2006).